Journal of the Korean Nuclear Society
Volume 31, Number 6, pp.561~571, December 1999

Microstructure and Mechanical Properties of Cr-Mo Steels for Nuclear Industry Applications

Sung Ho Kim, Woo Seog Ryu, and Il Hiun Kuk
Korea Atomic Energy Research Institute
150 Dukjin-dong, Yusong-gu, Taejon 305-353, Korea
shkim7@nanum.kaeri.re.kr

(Received June 4, 1999)

Abstract

Microstructure and mechanical properties of five Cr-Mo steels for nuclear industry applications have been investigated. Transmission electron microscopy, energy dispersive spectrometer, differential scanning calorimeter, hardness, tensile, and impact test were used to evaluate the Cr and W effect on the microstructure and mechanical properties. Microstructures of Cr-Mo steels after tempering are classified into three types : bainitic 2.25Cr-1Mo steel, martensitic Mod.9Cr-1Mo, HT9M, and HT9W steels, and dual phase HT9 steel. The majority of the precipitates were found to be $M_{23}C_6$ carbides. As minor phases, fine needle-like V(C,N), spherical NbC, fine needle-like Cr-rich Cr_2N, and Cr-rich M_7C_3 were also found. Addition of 2wt.% W in Cr-Mo steels retarded the formation of subgrain and dissolution of Cr_2N precipitates. Hardness and ultimate tensile strength increased with increasing Cr content. Though Cr content of HT9W steel was lower than that of HT9 steel, the hardness of HT9W was higher due to the higher W content. W added HT9W steel had the highest ultimate tensile strength above 600℃. But impact toughness of W added steel (HT9W) and high Cr steel (HT9) was low.

Key Words : Cr-Mo steel, carbide, tensile properties, hardness, impact, martensite

1. Introduction

Cr-Mo steels have been receiving attention for fuel cladding and duct applications in liquid metal reactor core components because of their excellent swelling resistance in comparison with austenitic stainless steels [1,2]. Cr-Mo steels have also been used in liquid metal reactor steam generator tubes because they have lower carbon activity, resistance to decarburization in sodium, good waterside corrosion resistance, resistance to waterside stress corrosion in the event of chloride caustic ingress, and resistance to stress corrosion cracking following a steam to sodium leak[3]. One of the most important challenges in fusion technology research and development is the development of low-activation materials. Presently, ferritic/martensitic steels, vanadium alloys and

SiC/SiC composite materials are considered promising candidates. Of these candidates, low activation ferritic/martensitic steels (Cr-Mo steels) are recognized as the most advanced and mature materials[4]. In order to use the Cr-Mo steels in nuclear industry, optimum balance between high fracture toughness, low ductile-to-brittle transition temperature (DBTT), and high creep rupture strength should be achieved. To increase the efficiency of power plant, higher creep strength is sought by increasing tempering resistance through the addition of elements such as Mo, W, V, Nb, etc.. To achieve the higher operating temperature, minimization of microstructural degradation is required, that is, the carbides formed by tempering must be resistant to growth during service, thereby providing microstructural stability.

In Cr-Mo steels the influence of alloying elements on properties is as follows. Carbon exists in the solid solution state after austenitization and precipitates as carbide during tempering treatment. Higher carbon content causes more carbide precipitation. These carbides easily coarsened during service. In that case, the precipitation hardening effect was lost. Carbon also consumed solid solution hardening elements such as Mo and W by forming carbides, so that the solid solution hardening effect was also lost. Carbon lowers the toughness and weldability, impairs corrosion resistance and requires a higher austenitizing temperature to dissolve the carbides, which would lead to coarse austenite grain sizes and a decrease creep ductility[5]. Thus it is desirable that the carbon content is preserved about 0.2wt.%. Mo and W are ferrite stabilizing elements, and act as solid solution hardening elements[6]. The addition of W retards the recovery of dislocation and recrystallization rate because W inhibits the diffusion of Fe atoms[7]. Mo and W may dissolve into $M_{23}C_6$ carbide, thus increase the thermal stability of this carbide and also increase the high temperature long-term creep rupture strength. It is desirable that the molybdenum equivalent ($Mo_{equi.}$) given by (Mo + 1/2W) is preserved below 1.5 to optimized the long term creep rupture strength and toughness[8]. Too much Mo and W reduced toughness by forming δ-ferrite and intermetallic compound (Laves phase). Nb and V are also ferrite forming elements and act as precipitation hardening element[9]. Vanadium finely precipitates as V(C,N) or V_3C_4 and partially dissolves into the matrix and $M_{23}C_6$. The optimum content of V is about 0.2wt.%. Nb is a strong carbide former. NbC is not dissolved after austenitizing at 1050℃. V and Nb precipitates do not coarsened during creep test and therefore improve the creep rupture strength. The Cr addition improves the corrosion and oxidation resistance, high temperature strength, and reduces toughness[10]. Ni and Mn are austenite stabilizers, which are added to inhibit the formation of δ-ferrite during austenitizing treatment.

In the present work, commercial Cr-Mo steels (2.25Cr-1Mo, Mod.9Cr-1Mo and HT9) and modified Cr-Mo steels (HT9M and HT9W) have been studied to evaluate the Cr and W effect on the microstructure and mechanical properties. These results may be used in the selection of materials for the advanced nuclear power plant and the development of the advanced materials.

2. Experimental Procedure

Five Cr-Mo steels were investigated ; their compositions are given in Table 1. Cr content varied from 2.25wt.% to 12wt.%. HT9W and HT9 steels contained W, 2.0wt.% and 0.5wt.%, respectively. 2.25Cr-1Mo steel was manufactured by Lukens, and the others were laboratory melted in a vacuum by an induction furnace. Four 30kg ingots, which were melted and hot rolled at 1150℃

Table 1. Chemical Compositions of Cr-Mo Steels (wt.%)

Cr-Mo steels	C	Si	Mn	Ni	Cr	Mo	V	Nb	W	N	remarks
2.25Cr-1Mo	0.10	0.19	0.41	0.2	2.18	0.96	0.007	0.003	-	-	Lukens
Mod.9Cr-1Mo	0.099	0.32	0.42	0.10	9.03	0.96	0.22	0.094	-	0.032	*
HT9M	0.145	0.1	0.45	0.46	9.79	1.23	0.2	0.18	-	0.02	*
HT9W	0.12	0.08	0.59	0.38	10.87	0.48	0.201	0.060	2.04	0.045	*
HT9	0.19	0.36	0.59	0.53	11.79	0.99	0.31	0.02	0.49	<0.01	*

*) VIM lab. melted

Table 2. Transformation Temperatures, $Cr_{equi.}$ and Heat Treatment Conditions

Cr-Mo steels	A_{e1}	A_{e3}	$Cr_{equi.}$	M_s	Austenitization	Tempering
2.25Cr-1Mo	800	843	1.67	-	905℃/20mim.	760℃/28mim.
Mod.9Cr-1Mo	850	885	9.56	360	1050℃/1hr	750℃/2hrs
HT9M	830	878	9.33	331	1050℃/1hr	750℃/2hrs
HT9W	854	902	10.66	321	1050℃/1hr	750℃/2hrs
HT9	866	909	11.27	350	1050℃/1hr	750℃/2hrs

to a final plate thickness of 15mm and 4mm. Heat treatment conditions of Cr-Mo steels are shown in Table 2.

Conventional optical and electron metallographic studies were carried out. Both extraction replica and thin foil electron microscopical techniques were employed. Carbon extraction replicas were prepared by initially etching the specimens in a 10% HF + 5% HNO_3 + 85% H_2O solution and stripping the replica in a solution of 10% HNO_3 and 2% HCl in methanol. The thin foils were prepared with a 25% HNO_3-methanol solution and were electropolished to perforation in a 10% HCl-methanol mixture at −40℃. A DSC (differential scanning calorimeter) and dilatometer were used to measure the A_{e1}(eutectoid temperature), A_{e3}(α-γ transformation temperature), and M_s (martensite transformation start temperature).

Determination of vickers microhardness was made at room temperature using a 500g load. Tensile specimens with a gage length of 25mm were cut from the 4mm thick sheet with longitudinal directions parallel to the rolling direction. Tensile tests were carried out at temperatures between room temperature and 700℃. Charpy V-notch impact tests were carried out at temperatures between -120℃ and +180℃. Standard Charpy V-notch specimens were machined with a LT orientation (notch vertical to the rolling direction). Ductile-to-brittle transition temperatures were taken as the temperatures corresponding to absorbed energies equal to 50J.

3. Results and Discussion

3.1 Microstructure

The experimentally measured A_{e1}, A_{e3}, and M_s values and the chromium equivalent ($Cr_{equi.}$) calculated using Schneider equation[11] are shown in Table 2. Cr-Mo steels are commonly used in austenitized and tempered conditions. Austenitization treatment should be carried out above A_3 for the complete transformation to austenite and the sufficient dissolution of carbides.

Tempering temperature should be below A_1 to avoid the formation of austenite during tempering. So the heat treatment conditions of Cr-Mo steels except 2.25Cr-1Mo steel are selected as follows ; austenitizing at 1050℃ for 1 hour and tempering at 750℃ for 2 hours.

Typical optical micrographs after tempering treatment are shown in Fig. 1. It can be seen that these are classified into three types : bainitic 2.25Cr-1Mo steel, martensitic Mod.9Cr-1Mo, HT9M, and HT9W steels, and dual phase HT9 steel. 2.25Cr-1Mo steel had bainitic structure due to low Cr content, but matrix of 9~12Cr-Mo steels was lath martensite. $Cr_{equi.}$ of HT9 steel is high enough to form δ-ferrite. So HT9 steel contained a small amount of δ-ferrite which was dispersed in the martensite phase. δ-ferrite can exert a detrimental effect on both toughness and ductility[6], although it can reduce austenite grain growth and at the same time increase creep rupture time and improve weldability and formability[12].

TEM microstructures of tempered Cr-Mo steels are shown in Fig. 2. In the austenitized condition, the microstructure consisted of bainite or lath martensite with a high dislocation density, together with undissolved carbides. As carbides started to precipitate, dislocation density reduced,

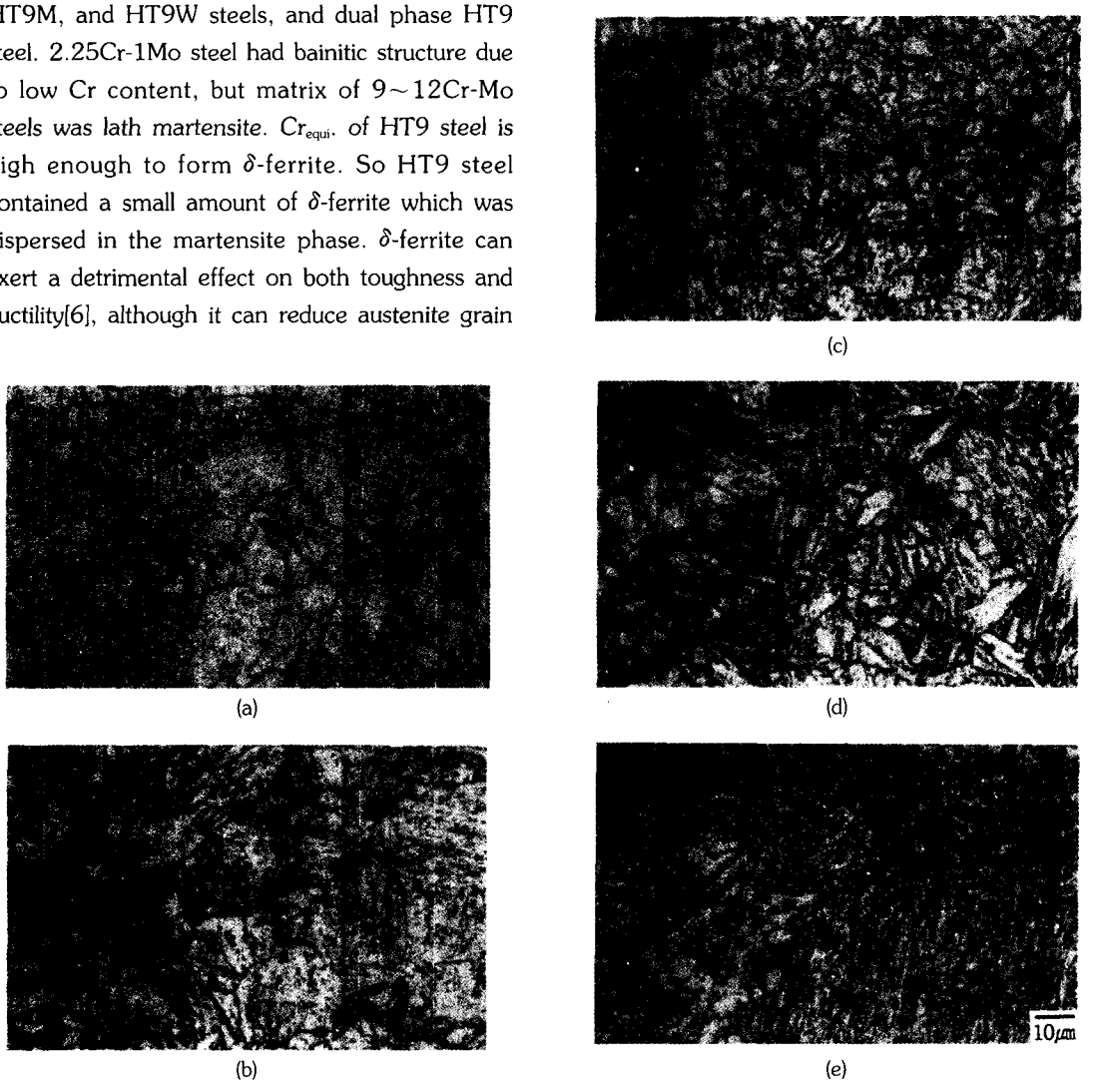

Fig. 1. Optical Micrographs of Cr-Mo Steels
(a) 2.25Cr-1Mo (b) Mod.9Cr-1Mo (c) HT9M (d) HT9W (e) HT9

and fine subgrains with low dislocation densities were formed with tempering treatment. The subgrain boundaries were frequently laid transverse to the principal direction of the martensite lath. The formation of subgrain was varied with Cr and W content. In 2.25Cr-1Mo steel, subgrains were completely formed and growth of subgrains occurred even though the tempering was carried out at lower tempering parameter [Larson-Miller parameter : $T(20+\log t(hr)) \times 10^{-3}$] than high Cr steels. And subgrains were only completely formed in Mod.9Cr-1Mo steel. On the other hand, subgrains were not yet completely formed in the high Cr steels (HT9M, HT9W, and HT9 steels) tempered at 750℃. Especially the formation of subgrains was retarded in W added HT9W steel compared with HT9M steel which did not contain W. Annihilation and redistribution of dislocation were retarded and formation of subgrains was also delayed because W inhibited the diffusion of Fe atoms. Thus the microstructural degradation of HT9W steel may be retarded during long service time at high temperature because W added steel can be tempered at higher temperature.

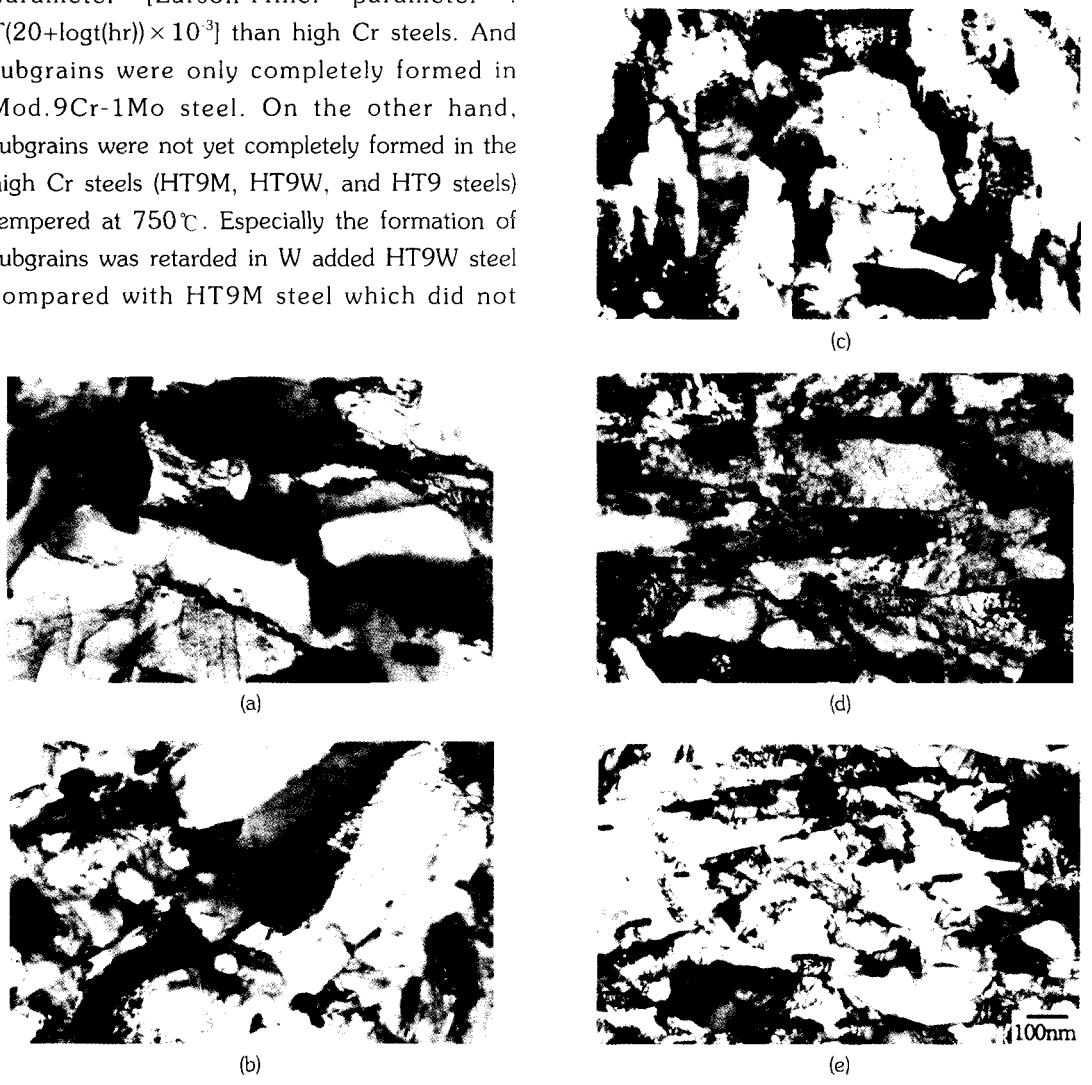

Fig. 2. TEM Microstructures of Cr-Mo Steels
(a) 2.25Cr-1Mo (b) Mod.9Cr-1Mo (c) HT9M (d) HT9W (e) HT9

3.2. Carbide Precipitation

Electron microscopy on carbon film extraction replicas was performed to identify and evaluate the precipitates. In normalized conditions, all carbides were dissolved except NbC. Carbides start to precipitate during tempering. As tempering temperature increased, precipitation reaction changed. That is, the equilibrium precipitation reactions changed.

In 2.25Cr-1Mo steel, the precipitation sequence is as follows[13] ;

matrix→M_3C→M_3C+M_2C→$M_{23}C_6$+ M_7C_3→M_6C

In 9-12Cr steels, the precipitation sequence is as follows[14] ;

matrix → M_3C → M_2X + $M_{23}C_6$ → $M_{23}C_6$ + MC

The majority of the precipitates in all Cr-Mo steels were found to be $M_{23}C_6$. These carbides were rich in chromium and iron, as shown in a typical energy dispersive spectrometer (EDS) spectrum given in Fig. 3. Small amounts of vanadium, molybdenum, and/or tungsten were also detected. In addition to $M_{23}C_6$, fine needle-like V(C,N) and spherical NbC were found in Mod.9Cr-1Mo, HT9M, and HT9W steels. The size of V(C,N) precipitates was of the order of 20

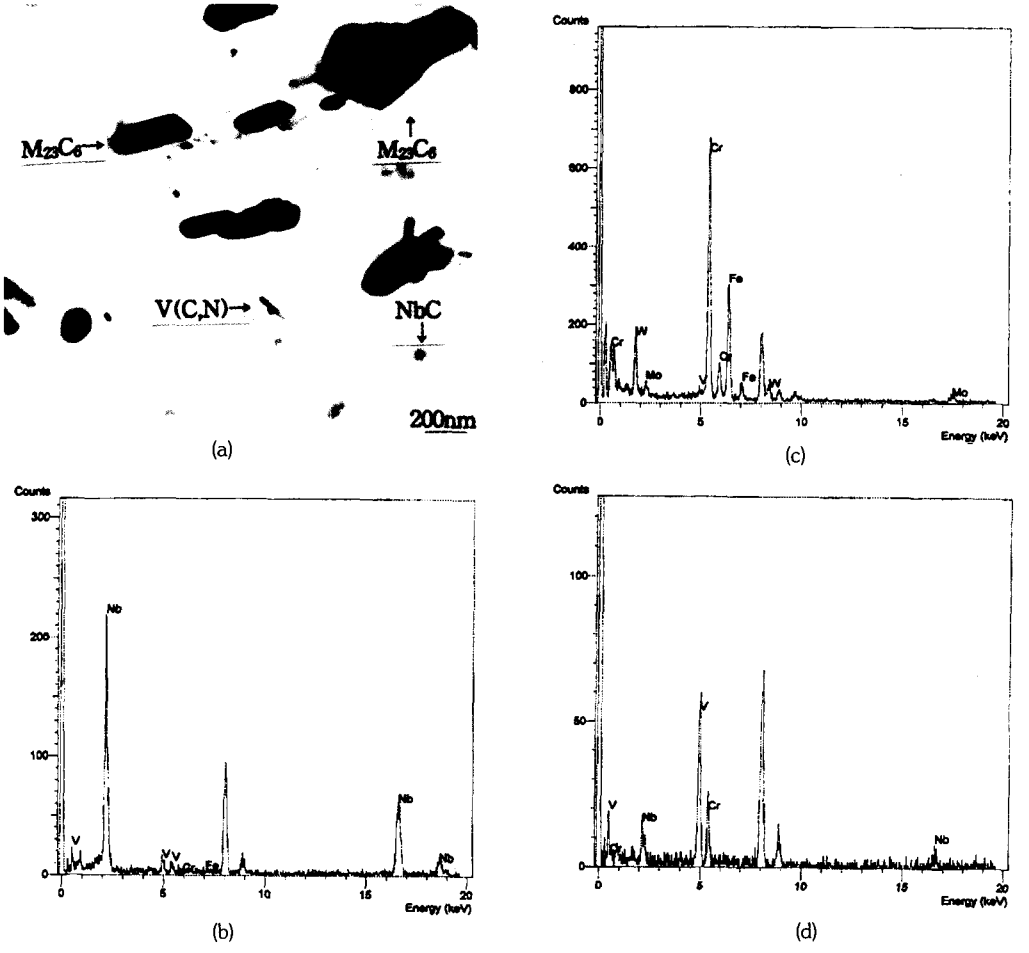

Fig. 3. Carbide Morphology (a) and EDS Results $M_{23}C_6$ (b) NbC (c) V(C, N) (d)

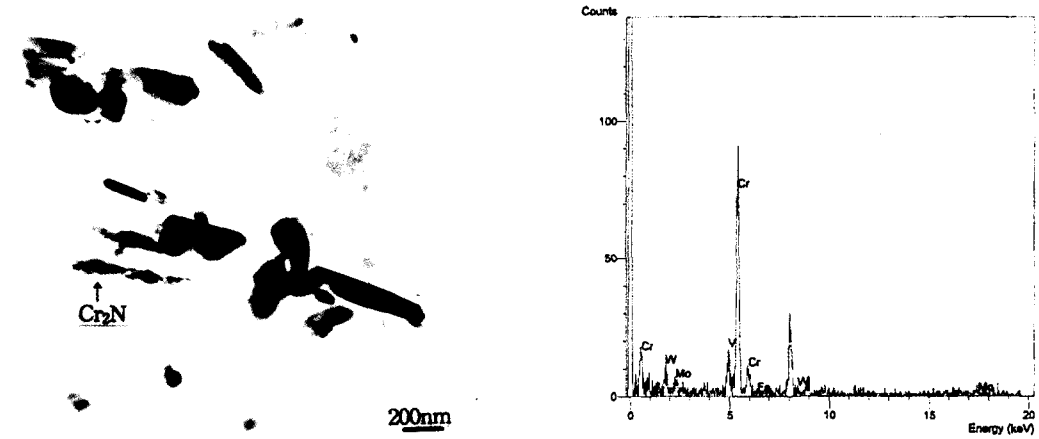

Fig. 4. Carbide Morphology and EDS Result of Cr-rich Cr_2N

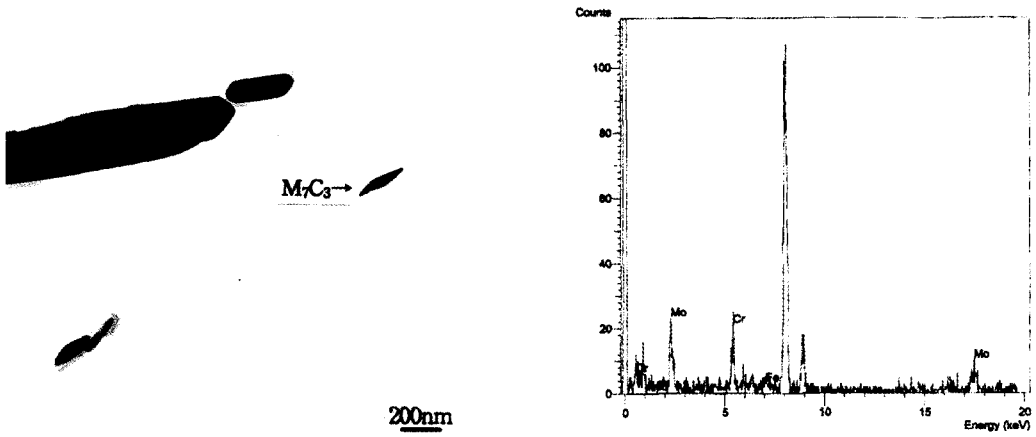

Fig. 5. Carbide Morphology and EDS Result of Cr-rich M_7C_3

Table 3. Minor Phases Present in the Cr-Mo Steels

Cr-Mo steels	Minor phases	Quantitative EDS results (at%)
2.25Cr-1Mo	$M_{23}C_6$, M_7C_3	$M_{23}C_6$: 67Fe-29Cr-4Mo, M_7C_3 : 52Cr-42Mo-6Fe
Mod.9Cr-1Mo	$M_{23}C_6$ NbC, V(C,N)	$M_{23}C_6$: 64Cr-31Fe-4Mo-1V, NbC : 87Nb-8V-5Cr, V(C,N) : 71V-17Cr-12Nb
HT9M	$M_{23}C_6$, NbC, V(C,N)	$M_{23}C_6$: 67Cr-29Fe-4Mo, NbC : 94Nb-4V-2Cr, V(C,N) : 77V-14Cr-9Nb
HT9W	$M_{23}C_6$, NbC (C,N), Cr_2N	$M_{23}C_6$: 63Cr-28Fe-2Mo-7W, NbC : 65Nb-14Cr-12V-9W V(C,N): 62V-21Cr-5Nb-12W, Cr_2N :74Cr-16V-6W-2Mo-2Fe
HT9	$M_{23}C_6$ NbC	$M_{23}C_6$: 66Cr-27Fe-3Mo-3W-1V MC : 84Nb-8V-4Cr-4W

Table 4. Vickers Microhardness

Cr-Mo	2.25Cr-1Mo	Mod.9Cr-1Mo	HT9M	HT9W	HT9
Hardness	200	226	259	282	276

$\times 200nm^2$ and the size of NbC precipitates was about 80nm in diameter. Also Cr-rich precipitates were found only in HT9W steel. This Cr-rich precipitates was identified as Cr_2N, which is shown in Fig. 4. Cr_2N was dissolved in other Cr-Mo steels tempered at 750℃. This showed that dissolution of Cr_2N was retarded in HT9W steels due to the addition of W. In 2.25Cr-1Mo steel, M_7C_3 precipitates were found (Fig. 5). Fine needle-like V(C,N) precipitates were not formed in HT9 steel because the nitrogen content was below 0.01wt.%. The minor phases and quantitative EDS results are summarized in Table 3.

$M_{23}C_6$ carbides are formed at prior austenite grain boundaries and subgrain boundaries. Cr_2N and V(C,N) are formed preferentially at dislocation or martensite lath boundaries. These carbides produced the basic creep strength of Cr-Mo steels by retarding subgrain growth. The NbC and M_7C_3 are precipitated within subgrains where they pin down free dislocations and therefore increase creep strength.

3.3. Microhardness

Table 4 shows the vickers microhardness values for Cr-Mo steels. The hardness test results showed that hardness value increased with increasing Cr content. But 2wt.%W added HT9W steel exhibited higher hardness value compared with HT9 steel which had a higher Cr content. 2.25Cr-1Mo steel exhibited the lowest hardness.

Microstructural degradation effects can take place during long service time at high temperature. These are the particle coarsening of the carbides and the growth of subgrains. Carbides, formed at high tempering temperatures, may be more stable phases and pin the boundaries and prevent subgrain growth. The slower the particle coarsening rate, the longer the time before unpinning of the subgrain growth. This pinning of the tempered martensite lath boundaries promotes microstructural stability and prevents the creep rupture strength from decreasing during extended service time. It is desirable that tempering treatment is performed at higher temperature to preserve microstructural stability during long service time. Because W added HT9W steel preserved the highest hardness value in the same tempering condition, it is possible that HT9W steel can be tempered at higher temperature than other Cr-Mo steels. So it is expected that the creep rupture strength of HT9W steel may be improved.

3.4. Tensile Properties

Tensile properties of Cr-Mo steels have been measured for test temperatures from room temperature to 700℃. A typical plot of ultimate tensile strength and yield strength against test temperature is shown in Fig.6. Ultimate tensile strength of higher Cr and carbon steels was higher than that of lower Cr and carbon steels. HT9 steel which contained the highest Cr and carbon content showed the highest ultimate tensile strength from room temperature to 600℃, but above 600℃, ultimate tensile strength of HT9 steel decreased rapidly, therefore HT9W steel exhibited the highest ultimate tensile strength. On the other hand, yield strength of HT9W steel was higher than that of HT9 steel at all test

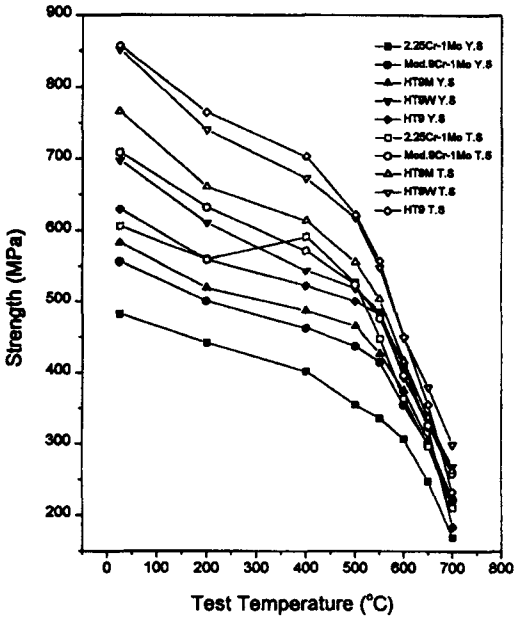

Fig. 6. Strengh of Cr-Mo Steels

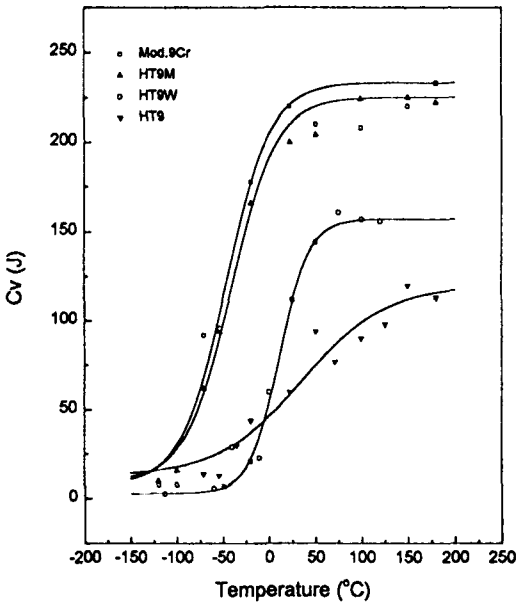

Fig. 8. Absorbed Energy of Cr-Mo Steels

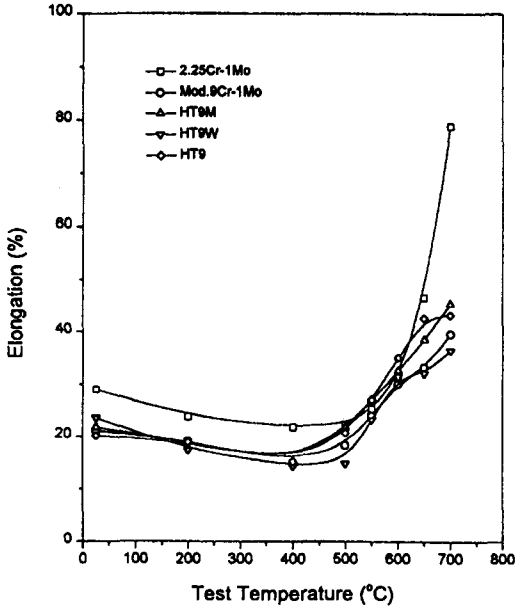

Fig. 7. Elongation of Cr-Mo Steels

temperatures. Total elongation is shown in Fig. 7. It can be seen that there is a minimum in the elongation curve at 400℃. 2.25Cr-1Mo steel exhibited the highest elongation and 9-12% Cr steels had no severe difference in elongation with Cr content.

3.5. Impact Properties

Fig. 8 shows the temperature dependence of the impact energy of Mod.9Cr-1Mo, HT9M, HT9W, and HT9 steels. Ductile-to-brittle transition temperatures (DBTT) at an impact energy of 50 joules were about -80℃ in Mod.9Cr-1Mo and HT9M steels and 0℃ in HT9W and HT9 steels. Upper shelf energies were about 230 joules in Mod.9Cr-1Mo and HT9M steels, 160 joules in HT9W steel, and 120 joules in HT9 steel. Lower shelf energies were similar in the four steels. The higher the yield strength, the lower the impact energy, but upper shelf energy is independent of yield strength[15]. The present works showed the similar results. The impact toughness of W added

steel (HT9W) was low because HT9W steel showed the highest yield strength at room temperature as shown in Fig. 6. Especially HT9 steel had the highest DBTT, because HT9 steel contained the small amount of δ-ferrite. The δ-ferrite has a lower toughness than martensite, and Laves phase and coarse $M_{23}C_6$ carbide precipitated along the δ-ferrite and matrix interface, cracks developed during the impact test were easily propagated along this interface[16]. Thus, charpy impact energy may be decreased when the δ-ferrite was contained.

4. Conclusions

Microstructure and mechanical properties of Cr-Mo steels for nuclear industry applications have been investigated. Following conclusions can be made ;

1. In 2.25Cr-1Mo steel, subgrains were completely formed and growth of subgrains occurred, but subgrains were not yet completely formed in the high Cr steels (HT9M, HT9W, and HT9 steels). Especially the formation of subgrains and the dissolution of Cr_2N were retarded in W added HT9W steels because the recovery of dislocation was delayed by the addition of W.
2. Hardness value increased with increasing Cr content, so 2.25Cr-1Mo steel had the lowest hardness value. But HT9W steel exhibited higher hardness value compared with HT9 steel which had a higher Cr and carbon content. The high temperature ultimate tensile strength also increased with increasing Cr and carbon content below 600℃. But HT9W steel had higher ultimate tensile strength above 600℃ than HT9 steel.
3. But impact toughness of W added steel (HT9W) and high Cr steel (HT9) was low.

Acknowledgement

This work has been carried out as a part of the reactor core materials research and integrated database establishment under the nuclear R&D program by the Korean Ministry of Science and Technology.

References

1. A.L. Pitner, S.L. Hecht and R.G. Trenchard, " Nonswelling Behavior of HT9 Alloy Irradiated to High Exposure", WHC-SA-1967-FP (1993).
2. F.A. Smidt, Jr., P.R. Malmbery, J.A. Sprague and J.E. Westmoreland, " Swelling Behavior of Commercial Ferritic Alloys, EM-12 and HT-9, As Assessed by Heavy Ion Bombardment", ASTM STP 611, 227 (1976).
3. C. Willby and J. Walters, "Material Choice for the Commercial Fast Reactor Steam Generators", Pro. Inter. Conf. Ferritic Steels for Fast Reactor Steam Generator, p. 40, BNES, London (1978).
4. K. Ehrlich and S. Kelzenberg, H.D. Rohrig, L. Schafer and M. Schirra, " The Development of Ferritic-Martensitic Steel with Reduced Long-term Activation", *Journal of Nuclear Materials*, **212-215**, 678 (1994).
5. F.B. Pickering, "Historical Development and Microstructure of High Chromium Ferritic Steels for High Temperature Applications", Microstructural Development and Stability in High Chromium Ferritic Power Plant Steels, Ed. by A. Strang & D.J. Gooch, p. 1, The Institute of Materials, (1997).
6. K. Hashimoto, M. Yamanaka, Y. Otogura, T. Zaizen, M. Onoyama and T. Fujita, "Newly Developed 9Cr-2Mo-Nb-V(NSCR9) Steel", Proc. Topical Conf. Ferritic Alloys for use in Nuclear Energy Technologies, ed. by J.W. Davis and D.J. Michel, p. 307, The

Metallurgical Society of AIME, Utah (1983).
7. F. Abe, H. Araki and T. Noda, "The Effect of Tungsten on Dislocation Recovery and Precipitation Behavior of Low-Activation Martensitic 9Cr Steels", *Metallurgical Transactions A*, **22A**, 2225 (1991).
8. S. Shikakura, S. Nomura, S. Ukai, I. Seshimo, Y. Kano, Y. Kuwajima, T. Ito, K. Tutaki and T. Fujita, "Development of High-Strength Ferritic/Martensitic Steel for FBR Core Materials", *Journal of The Atomic Energy Society of Japan*, **33**, 1157 (1991).
9. T. Fujita, "Development of High Chromium Ferritic Steels for Ultra Super Critical Power Plant", *Journal of The Iron and Steel Institute of Japan*, **76**, 1053 (1990).
10. N. Abe, T. Ikoma and M. Tamura, *Transactions Iron and Steel Institute of Japan*, **24**, (1984).
11. H. Schneider, *Foundry Trades J.*, **108**, 562 (1960).
12. R.S. Fidler and D.J. Gooch, "The Hot Tensile Properties of Simulated Heat Affected Zone Structures in 9CrMo and 12CrMoV Steels", Pro. Inter. Conf. Ferritic Steels for Fast Reactor Steam Generator, p. 128, BNES, London (1978).
13. R.G. Baker and J. Nutting, *Journal of the Iron and Steel Institute*, **192**, 257 (1959).
14. K.J. Irvine, D.J. Crowe and F.B. Pickering, *Journal of the Iron and Steel Institute*, **195**, 386 (1960).
15. E.A. Little, D.R. Harries and F.B. Pickering, "Some Aspect of the Structure-Property Relationships in 12% Cr Steels", Proc. Int. Conf. Ferritic Steels for Fast Reactor Steam Generators, ed. by S.F. Pugh and E.A. Little, p. 136, British Nuclear Energy Society, London (1978).
16. A. Iseda, H. Teranishi and K. Yoshikawa, "Effect of Silicon and Molybdenum on Long-term Heating Embrittlement and Precipitation of Laves Phase of High Chromium Ferritic Heat Resistance Steels", *Journal of The Iron and Steel Institute of Japan*, **76**, 2190 (1990).